# Wear performance of quenched wear resistant steels in abrasive slurry erosion

Niko Ojala[1](*), Kati Valtonen[1], Atte Antikainen[1], Anu Kemppainen[2], Jussi Minkkinen[3], Olli Oja[3] and Veli-Tapani Kuokkala[1]

[1]Tampere University of Technology, Department of Materials Science, Tampere Wear Center, Tampere, Finland
[2]SSAB Europe Oy, Raahe, Finland
[3]SSAB Europe Oy, Hämeenlinna, Finland

[*]Corresponding author: Niko Ojala; Tampere University of Technology, Department of Materials Science, P.O.Box 589, FI-33101 Tampere, Finland; tel. +358 50 317 4516; email niko.ojala@tut.fi

## ABSTRACT

Three commercially available quenched wear resistant steel grades were compared with a structural steel and four elastomer materials to reveal the differences in their behavior in slurry erosion conditions and to find the best solutions for demanding applications. A slurry-pot tester, allowing simulation of various wear conditions with different minerals, particle sizes (up to 10 mm), abrasive concentrations, and sample angles was used to simulate different industrial slurry applications. In this study, granite and quartz with concentrations of 9 and 33 wt% were used as abrasives in tests conducted at 45° and 90° sample angles. The performance of the studied steels was evaluated with respect to their material properties such as hardness and microstructure. Furthermore, the cross-sections and wear surfaces of the test samples were analyzed to reveal the possible differences in the mechanical behavior of the materials during slurry erosion. The wear surface analyses show that abrasion is the dominating wear mechanism already for the smallest particle size of 0.1/0.6 mm. In low-stress abrasive slurry erosion with the smallest particles, the elastomers showed better wear resistance than the steels, whereas in demanding high-stress abrasive slurry erosion conditions the quenched wear resistant steels can well compete with elastomers in wear resistance. The relative wear performance of the steels increased with increasing abrasive size, while for the elastomers it decreased.

Keywords: Slurry erosion; Wear testing; Steel; Elastomers; Mining, mineral processing

# 1. INTRODUCTION

Slurry is generally defined as a mixture of liquid and solid particles that can be transported by pumping. Transporting minerals or moving solids as a slurry is an increasingly viable alternative in many industrial applications ranging from dredging and pumping concrete at a construction site to large mining projects. In mines the slurry transportation of minerals is both an economical and environmentally friendly alternative, whereas for transferring concrete to its destination at large construction sites, pumping is generally the only option. The main factor related to the expenses of such pumping projects is wear. The wear environment, including mechanical wear and corrosion, dictates the initial capital costs and useful lifetime of the pipelines. [1–4] Size of the particles inside the slurry is one of the major factors affecting the wear in the process. In heavy duty slurry pumping the particle size can be up to several centimeters [5], while in fine particle mineral processes the particle sizes are typically between 100 and 250 micrometers [6,7].

Wear related problems cause significant economic and environmental losses in applications involving abrasive and erosive wear, such as pumps and pipelines in slurry transportation or pumps and crowns in dredging. Mainly due to corrosion, quenched wear resistant steels are not widely used in piping. However, the good mechanical wear resistance that steels can offer may have a greater effect on the pipe lifetime than their relatively poor corrosion resistance, when highly abrasive slurries are handled. The particles in the slurry can be large and sharp and the speed of the flow high, causing abrasive slurry erosion. In these conditions, understanding the active wear mechanisms is essential for the use and further development of new materials.

The slurry pipeline technology is relatively young. The first slurry pipeline was implemented in the 1960's and the first long distance pipeline in the 1990's [2]. Currently elastomer lining materials, such as rubbers or polyurethanes, have become a standard choice for combined wear and corrosion protection in slurry pipelines transporting minerals. However, such linings can be rather expensive and also quite sensitive to surface defects. In addition, they are known to suffer from problems related to adhesion and thermal expansion in pumping and pipeline transport applications, which all will promote mechanical wear. For example for polyurethanes, Zhang et al. [8] suggested a two times increase in the erosion rate from room temperature to 60 °C, and a three times increase to 100 °C. Furthermore, as the trend is towards higher production volumes and slurry transportation is also expanding into new application areas possibly with coarser particles, mechanical wear resistance is becoming more and more important [2].

In very demanding pumping or transporting applications abrasive wear becomes even more dominant, as the high flow speed of the slurry and high abrasiveness of the particles inside the slurry leads to a subtype of slurry erosion called abrasive slurry erosion [9,10]. Currently in the industrial field the fine particle slurry pumping represents the low-stress abrasive slurry erosion, whereas dredging and large particle slurry pumping represents the high-stress abrasive slurry erosion. Only few publications have been published about the latter conditions, i.e., abrasive slurry erosion caused by large particles [9,11]. Additionally, it has been shown that with such also the role of corrosion becomes smaller [12,13]. Such a change in the wear environment requires new material solutions and in-depth research to better understand the wear mechanisms and performance of different materials.

Amongst the published studies related to the slurry erosion of steels [13–23], just a few have included quenched steels, and only two articles were found where steels had been compared with elastomers. Clark and Llewellyn [14] compared several commercial plate and pipe steels using fine particles and zero degree sample angle. In these tests, the steels were ranked according to their surface hardness, the best wear performance being obtained with the hardest steel. Xie et al. [23] compared steels and elastomers, as well as some other material types, using fine particles and different low-stress wear test devices. They concluded that during slurry transportation the impact angles of the particles are random and that with fine particles and low-stress conditions elastomers have an excellent wear resistance. Madsen [21] compared elastomers and metal alloys both in laboratory and in-service conditions. He concluded that with fine quartz slurry the elastomers have an advantage over the tested metals, but in the field studies white cast iron was the best or on par with the elastomers. Also wear resistant steels were in the field tests often better than elastomers.

Considering all the aforementioned and the results of Stachowiak and Batchelor [24], showing that the change in the particle size, even from very fine particles of 9 µm to fine particles of 127 µm, can cause fundamental changes in the wear mechanisms, it is worthwhile to study the slurry erosion performance of the quenched wear resistant steels and to compare them with the current wear resistant elastomers using an application oriented test method in test conditions ranging from low-stress abrasive slurry erosion with fine abrasive particles to high-stress abrasive slurry erosion with larger particles.

Gupta et al. [18] have shown that the pot testers are suitable for predicting slurry erosion in the in-service applications. They used a whirling arm slurry-pot, where two vertical samples were on the same level, to compare the results from laboratory studies to the results obtained from a 60 m long slurry pipeline pilot plant. They used different slurry concentrations, ranging from 15 to 45 wt%, and velocities of 4-8 m/s with particle sizes less than 0.5 mm, to compare the wear performance of brass (hardness 120 HV) and mild steel (hardness 160 HV) in both test environments. They concluded that the slurry-pot can be successfully used to simulate a pipeline application. However, they did not include any harder steels or larger particles sizes in their study.

In this work, three commercially available quenched wear resistant steel grades were compared with a structural steel and four elastomer materials to reveal the differences in their behavior in abrasive slurry erosion conditions and to find the best solutions for demanding applications. A slurry-pot tester was used as it allows the simulation of various wear conditions with different minerals, particle sizes and slurry concentrations in different industrial applications. The performance of the steels was evaluated with respect to the material properties such as hardness and microstructure. Furthermore, the cross-sections and wear surfaces of the test samples were analyzed to reveal the possible differences in the mechanical behavior of the test materials during abrasive slurry erosion.

# 2. MATERIALS AND METHODS

Application oriented wear tests with the high speed slurry-pot wear tester [9] at the Tampere Wear Center were performed for four steel and four elastomer materials. In this study, the test parameters were selected to simulate demanding industrial slurry applications, such as dredging and slurry transportation.

The primary test materials were three quenched wear resistant steels with hardness grades of 400, 450 and 500 HB. A 355 MPa structural steel, with hardness of 180 HV, was also tested as a reference material. Table 1 presents the measured surface hardness values, and the other mechanical properties as typical values and nominal compositions of the tested steels reported by the manufacturer. The nominal alloying of the untempered quenched steels was similar, as seen in Table 1. In the tests, a natural rubber with 40 shA hardness and three polyurethanes with hardness in the range of 75-90 shA represented the currently used materials in the slurry transportation applications and were therefore selected as comparison materials for the quenched steels. The tested polyurethanes are also available for slurry pump wear protection. Table 2 presents the typical mechanical properties of the tested elastomers and details of the polyurethanes reported by the manufacturer.

Fig. 1 presents the microstructures of the steels. The structural steel has a ferritic-pearlitic microstructure, whereas all of the wear resistant steels have an auto-tempered martensitic microstructure [25] with rather similar structure between all of them. The lath structures were well visible in the optical microscope revealing that the 400HB steel had the finest grain size. The quenched steels also contained a small portion of untempered white martensite, which is seen as unetched white areas in the micrographs.

The steel samples were 6 mm thick, while the elastomer samples were composed of a 6 mm elastomer coating over a 4 mm steel backing plate. The plate size was 64 x 40 mm. The elastomer plate samples were cut to shape so that the elastomer coating covered also one sample side to prevent wear of the base plate. For the 90° samples, this side was the sample tip (40 mm side), while for the 45° samples it was the leading edge (64 mm side).

**Table 1 Mechanical properties and nominal compositions of the studied steels**

| Material | 355 MPa | 400 HB | 450 HB | 500 HB |
|---|---|---|---|---|
| Hardness [HV10, kg/mm2] | 180 ±3 | 405 ±3 | 475 ±11 | 560 ±10 |
| Yield strength [N/mm$^2$] | 355 | 1000 | 1200 | 1250 |
| Tensile strength [N/mm2] | 470-630 | 1250 | 1450 | 1600 |
| A5 [%] | 20 | 10 | 8 | 8 |
| Density [g/cm$^3$] | 7.8 | 7.85 | 7.85 | 7.85 |
| C [max%] | 0.12 | 0.23 | 0.26 | 0.3 |
| Si [max%] | 0.03 | 0.8 | 0.8 | 0.8 |
| Mn [max%] | 1.5 | 1.7 | 1.7 | 1.7 |
| P [max%] | 0.02 | 0.025 | 0.025 | 0.025 |
| S [max%] | 0.015 | 0.015 | 0.015 | 0.015 |
| Cr [max%] | - | 1.5 | 1 | 1 |
| Ni [max%] | - | 1 | 1 | 1 |
| Mo [max%] | - | 0.5 | 0.5 | 0.5 |
| B [max%] | - | 0.005 | 0.005 | 0.005 |

**Table 2 Typical properties of the studied elastomers**

| Material | NR | PU1 | PU2 | PU3 |
|---|---|---|---|---|
| Hardness [ShA] | 40 | 75 | 85 | 90 |
| Tensile strength [N/mm2] | 25 | 23 | 42 | 37 |
| Density [g/cm$^3$] | 1.04 | 1.05 | 1.21 | 1.11 |
| Isocyanate type | - | MDI | MDI | TDI |
| Polyol type | - | polyether | polyester | polyether |

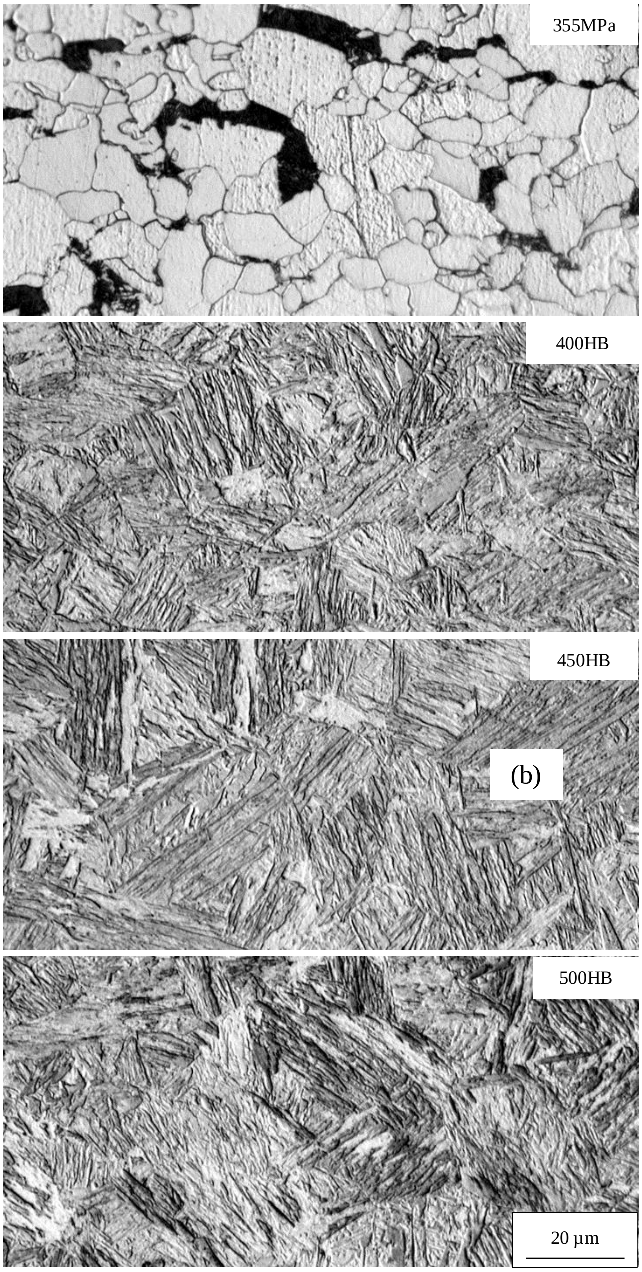


**Fig. 1 Optical micrographs of the studied steels**

The used test device is based on the pin mill type sample arrangement, where samples are attached to the main shaft at different vertical levels. The ‘pin mill’ name originates from industrial mineral refinement mill where steel pins are attached similarly to a vertical rotating shaft [9]. In the current tests, two lowermost sample levels were used. Fig. 2 shows the sample arrangement in the tester with steel plate samples at the two applied sample angles, 45° and 90°. For the test, the shaft with the samples is first lowered into the pot and then the slurry is added. In the current tests, the samples were spun in the pot at 1500 rpm for the total of 20 minutes. Each test consisted of four similar 5 minute cycles with the sample rotation method [9], which means that between every cycle the levels of the samples were switched and the slurry was replaced, e.g. sample that is first placed on upper level for first 5 minutes, was switched to lower level for second 5 minutes and so forth. The wear rates were determined by weighing the samples after each test cycle and then dividing the obtained values by the measured densities of the samples. The used abrasives were collected and sieved from the first half of each test, i.e., after first two test cycles, for analyzing the comminution of the abrasive particles.

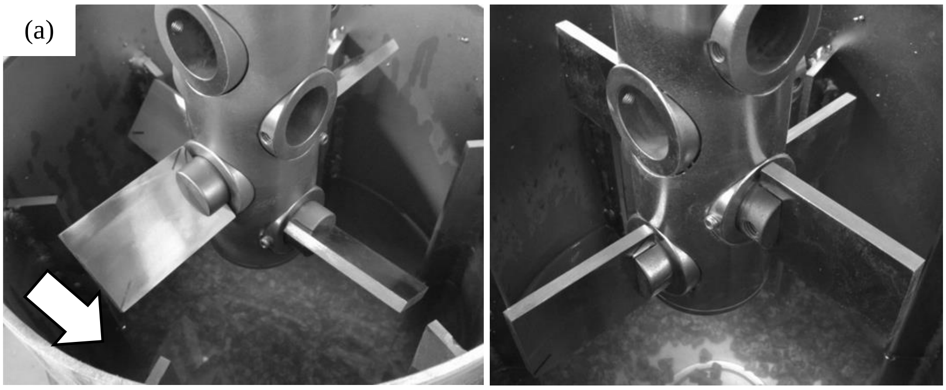


**Fig. 2 Sample arrangements with a) +45° (the arrow indicates the direction of rotation) and b) 90° sample angle**

Table 3 presents the test program, including two different minerals with different particle sizes and slurry concentrations, and two sample angles.  The program was designed to simulate abrasive erosion conditions, so the sample speed was selected to be high, from high-stress abrasive erosion, i.e., with slurry containing large granite particles, to low-stress abrasive erosion, i.e., with slurry containing fine particle size quartz. The granite gravel was acquired from Sorila quarry, Finland, and the quartz sand from Nilsiä quarry, Finland. The average hardness of the granite particles is 800 HV, while the quartz particles have an average hardness of 1200 HV. In many practical applications steels and elastomers are used as alternatives to each other, and therefore also in this study they were tested separately in the slurry-pot. This ensures that the different elastic responses of the two different material types in the slurry flow will not affect the results of the other type of a material. The 45 and 90 degree sample angles were selected to simulate the different contact conditions in slurry pumping, dredging and pipelines.

In the small particle slurry applications, the particle size normally is below 1 mm, but can also reach up to 10 mm, while the slurry concentrations can be up to 50-70 wt%, limited only by the rheological properties of the slurry. The slurry flow speed can vary between 10 and 25 m/s. [26] In the large particle applications, for example dredging pumps, up to 50 mm in particle size, the concentrations are typically much lower, down to 10-20 wt%, and the speeds are high, up to 30 m/s [27]. For example, in dredging, the concentrations and particle sizes can vary markedly during use. An additional fact is that inside the pot tester the flow patterns are turbulent , which means that the method simulates even better the practical slurry applications by offering a wide distribution of particle impact angles subjected on the wear test samples, still keeping the test environment sufficiently controlled for reproducible slurry erosion tests [9].

**Table 3 Test parameters used in the current tests**

<table>
<tr><th>Abrasive</th><th>Particle size [mm]</th><th>Slurry concentration [%]</th><th>Sample angle [°]</th><th>Sample tip speed [m/s]</th><th>Test time [min]</th></tr>
<tr><td rowspan="4">Granite</td><td>8/10</td><td rowspan="2">9</td><td>90</td><td rowspan="6">15</td><td rowspan="6">4 x 5</td></tr>
<tr><td>8/10</td><td rowspan="5">+45</td></tr>
<tr><td>8/10</td><td rowspan="4">33</td></tr>
<tr><td>2/4</td></tr>
<tr><td rowspan="2">Quartz</td><td>2/3</td></tr>
<tr><td>0.1/0.6</td></tr>
</table>

The samples were cut to shape by water cutting for minimizing any alterations in the sample properties. The surfaces of the steel samples were ground to remove the possible decarburization layer, after which the surface hardness of the samples was measured from the test surface. The wear surfaces and the cross-sections of the steel samples were characterized by both optical and scanning electron microscope (SEM, Philips XL 30). The wear surfaces were analyzed also with an optical 3D-profilometer (Alicona InfiniteFocus G5), and the microhardness values of the cross-sections were determined with a microhardness tester. With SEM, both secondary electron (SE) and backscatter electron (BSE) detectors were used, the SE images revealing better the surface topography and BSE images the embedded abrasive particles. Nital was used for etching of the steel samples. The elastomer samples were characterized using optical microscopy.

# 3. RESULTS

Fig. 3 presents the wear test results for the test materials, clearly indicating a change in the intensity of slurry erosion with the change in the wear environment. The large granite particles, even at low concentrations, induce much more abrasive slurry erosion in the elastomer materials than the fine quartz particles.  For the quenched steels, the wear rates are rather similar for the low concentration large particle (8/10 mm) and high concentration fine particle (0.1/0.6 mm) slurries, although the wear mechanisms are different. At 90° sample angle, the ductile elastomers withstand direct impacts well. However, the 45° sample angle inflicts more cutting on the wear surfaces, and the performance of the elastomers is notably decreased. With 8/10 mm granite abrasives, the order in the performance is the same for all three test parameters, the quenched steels being overall the best and the natural rubber being the best of the elastomers. With medium sized particles, the two softest elastomers, NR and PU1, are on a par with or even better than the steels. Furthermore, all elastomers show clearly lower wear rates compared to the steels when tested with fine quartz particles.

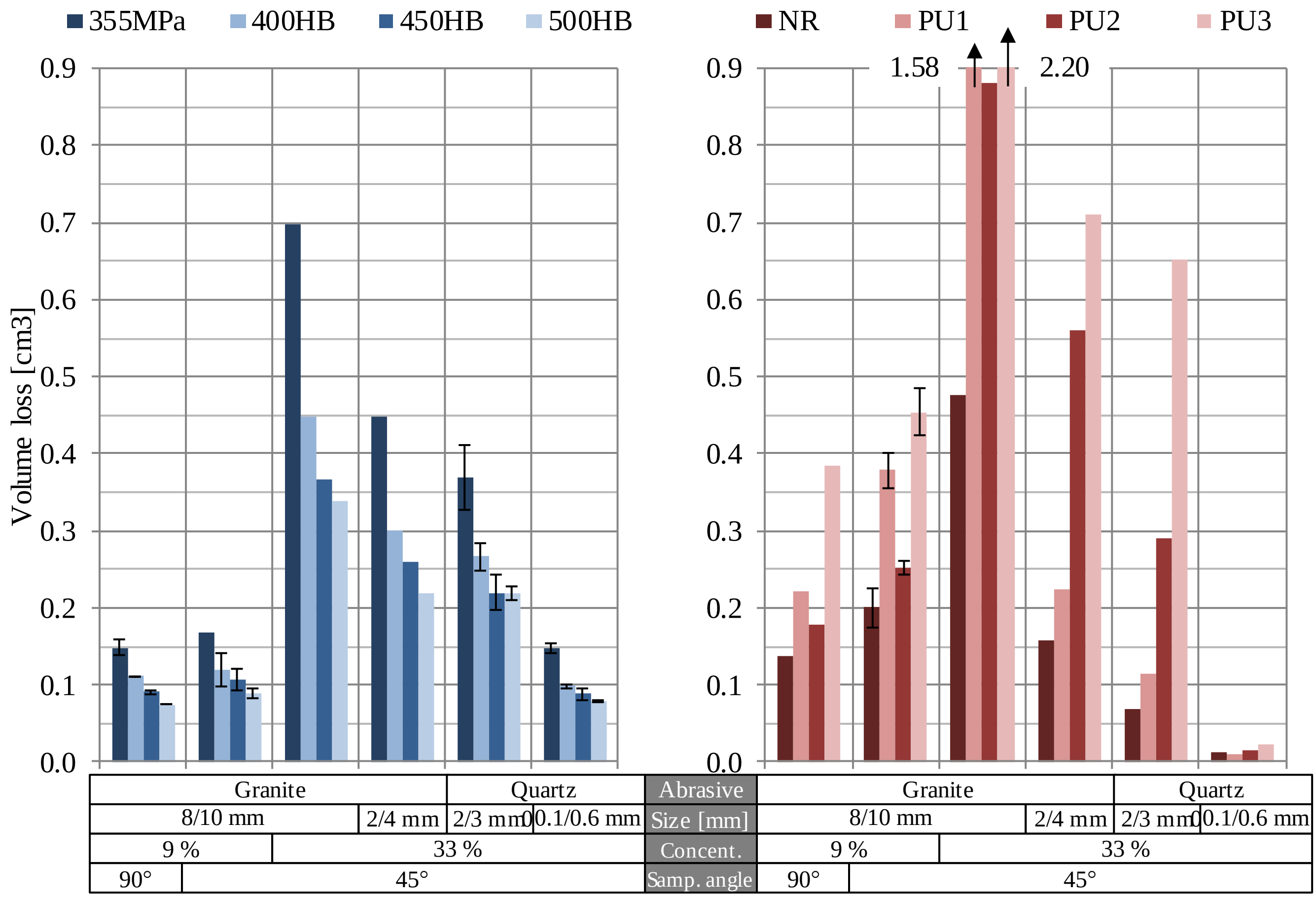


**Fig. 3 Wear test results for all test parameter and material combinations**

Fig. 4 presents the volume losses of the examined steels as a function of surface hardness when tested with different abrasives at the 45° sample angle and 33 % slurry concentration. It is notable that the volume losses decrease in a linear manner with every test parameter. The low concentration 8/10 mm granite showed similar linearity, but these results are excluded from the figure for clarity. Furthermore, the decrease was greater towards more abrasive conditions, i.e., in the figure the trend line slope for 8/10 mm granite is over five times steeper than that for 0.1/0.6 mm quartz.

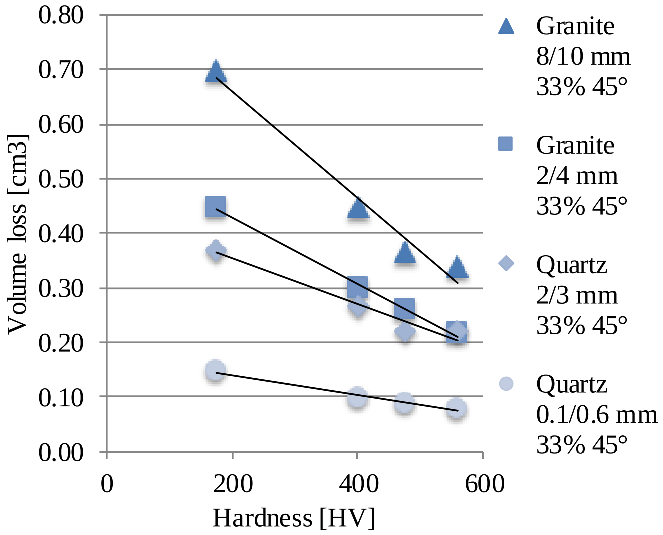


**Fig. 4 Volume loss as a function of surface hardness with different abrasives at 45° sample angle and 33 % slurry concentration**

## 3.1. Comminution of the abrasives

As the steels and elastomers were tested separately in groups of four samples, the comminution of the abrasives were analyzed after each test. Fig. 5 presents the comminution data for different abrasive types used in the tests. And Fig. 6 displays all abrasives before and after testing. It is notable that coarse quartz (2/3 mm) is comminuted more than the similar sized granite gravel because quartz is a more brittle rock. Crushability, indicating how easily a mineral can be crushed to smaller pieces, for quartz is 74 %, while for granite it is 34 %, and similarly, uniaxial compressive strengths are 90 and 194 MPa, respectively [28]. In contrast, fine quartz (0.1/0.6 mm) was basically not comminuted at all. With large granite (8/10 mm) and coarse quartz (2/3 mm), some differences were observed between the steels and the elastomers. These differences most likely arise from the different elastic responses of the materials in the slurry flow during the test. This means that the test conditions in those tests were not completely the same for both material types, but it is noteworthy that the differences are originating from the materials themselves, thus making the conditions realistic in relation to industrial applications.

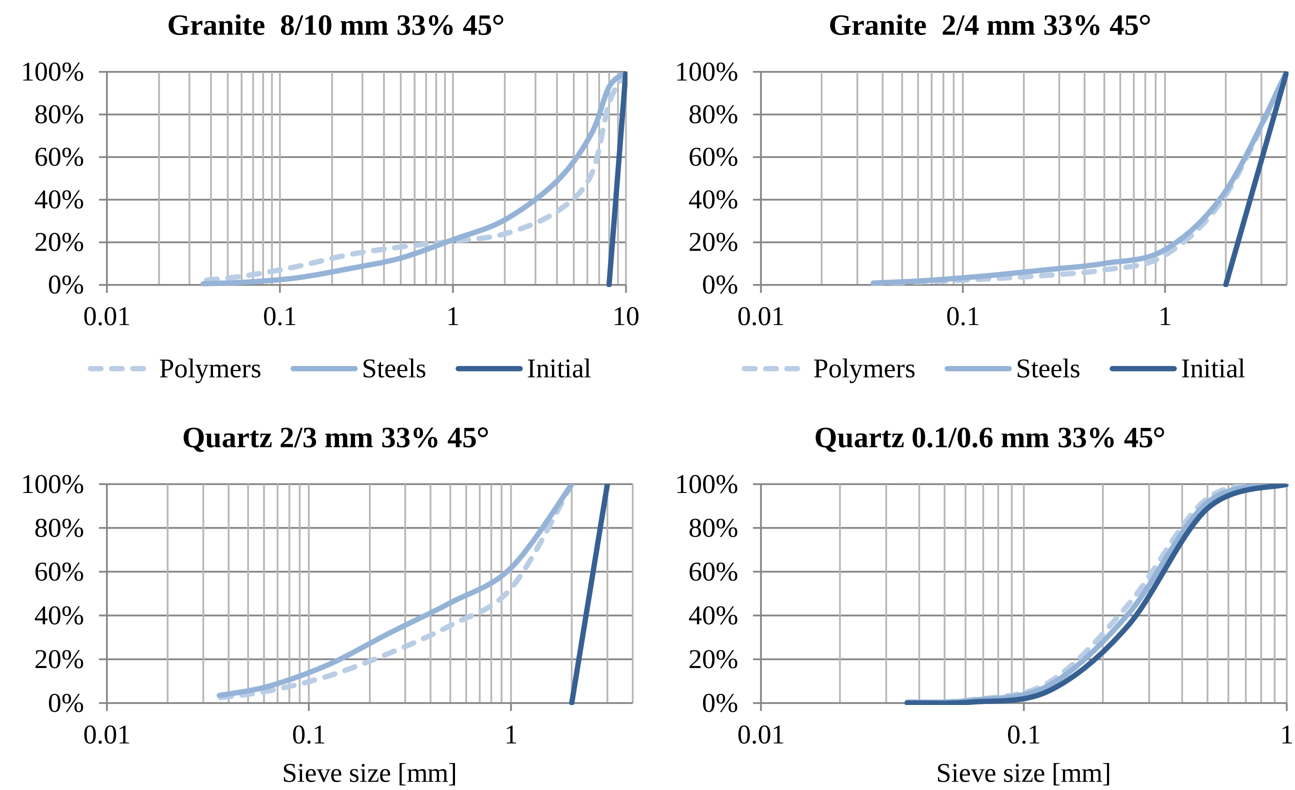


**Fig. 5 Cumulative sieving results of the used abrasives for different abrasive types**


**Fig. 6 Tested 355 MPa steel sample, and unused abrasives on upper row and the same after the test below**

## 3.2. Wear surfaces

All wear surfaces were characterized with optical microscopy and the quenched steels also with SEM. The sample edges were the most deformed places in the test samples. In the steels, wear causes plastic deformation, the extent of which depends on the strength, hardness and deformability of the steel. Fig. 7 shows the difference in the plastic deformation between the 450HB and 350MPa steels, both tested with 9 wt% 8/10 mm granite slurry using the 90° sample angle. In general, the structural steel samples were clearly more rounded than the quenched steel samples. Except for the smallest abrasive size, small burs going over the edges of samples' front surfaces, such as seen in Fig. 7, were observed. However, at the end of the tests there were no extensive burrs remaining in either of the materials, obviously because they had been cut away by the turbulent flow of slurry over the edges.

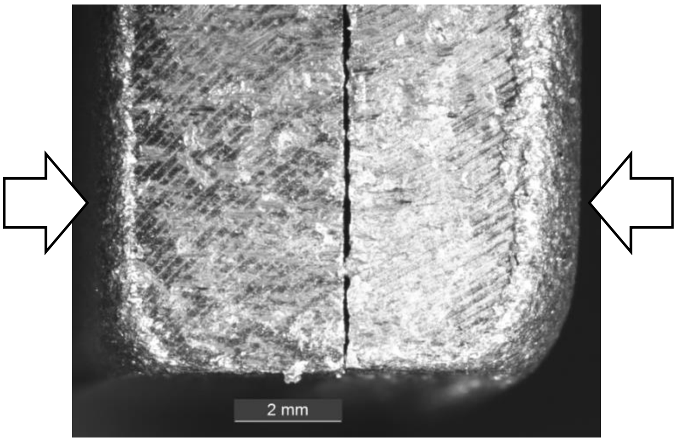


**Fig. 7 Deformation and rounding of the sample tip. On the left the 450HB and on the right the 355MPa steel, both tested with 9 wt% 8/10 mm granite slurry at the 90° sample angle. The arrows indicate the wear surfaces and the direction of the slurry flow**

The orientation of the wear marks on the surfaces of the steel samples depends on the sample angle. With the 90° sample angle, the orientation is slightly towards the upper corner of the plate sample, while with the 45° sample angle it is almost directly towards the upper edge of the sample. There is also a clear difference in the type of deformation and both the degree and amount of cutting, the 45° sample angle causing more deformation by ploughing and scratching. Fig. 8 presents the 400HB steel tested with both sample angles, clearly showing the differences in the wear mark orientation as well as in the type of deformation. In all wear surface images, the samples are positioned so that the sample tip is on the left hand side (see Fig. 2).

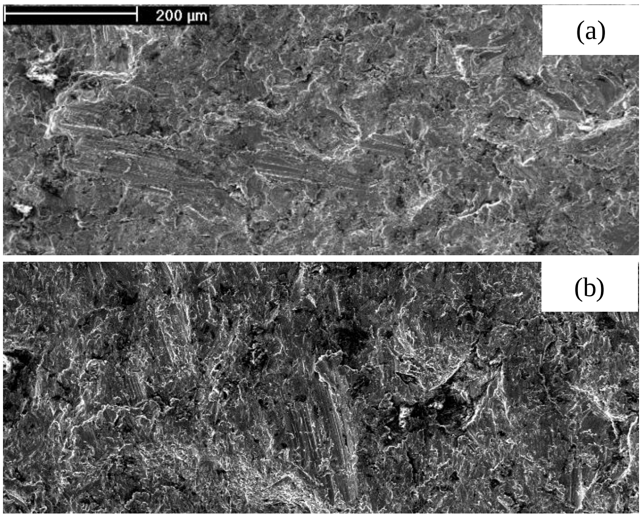


**Fig. 8 SEM images of the 400HB steel wear surfaces tested with 9 wt% 8/10 mm granite slurry at a) 90° and b) 45° sample angle. Images are taken from the bottom corner and 2 mm away from the sample tip**

With larger, over 2 mm particle sizes, the wear surfaces of the steels were covered by plastically deformed material in several stages of evolution. Individual impact-erosion wear features, such as small impact craters, embedded abrasive particles and short scratch marks, were found all over the surfaces. As erosion wear deforms the surface continuously, long or wide scratches are rare. With the smallest abrasive size, visible scratch marks were substituted by small scale scratches, and also the plastic deformation seemed to be limited.

Fig. 9 presents a wear surface comparison of the 33 wt% concentration 45° sample angle tests of the 400HB steel with different abrasives. The difference between the samples tested with fine quartz sand and the coarser abrasives is clear, while 2/4 mm granite and 2/3 mm quartz samples are almost identical. The largest abrasives caused largest deformations and widest scratches, as could be expected.

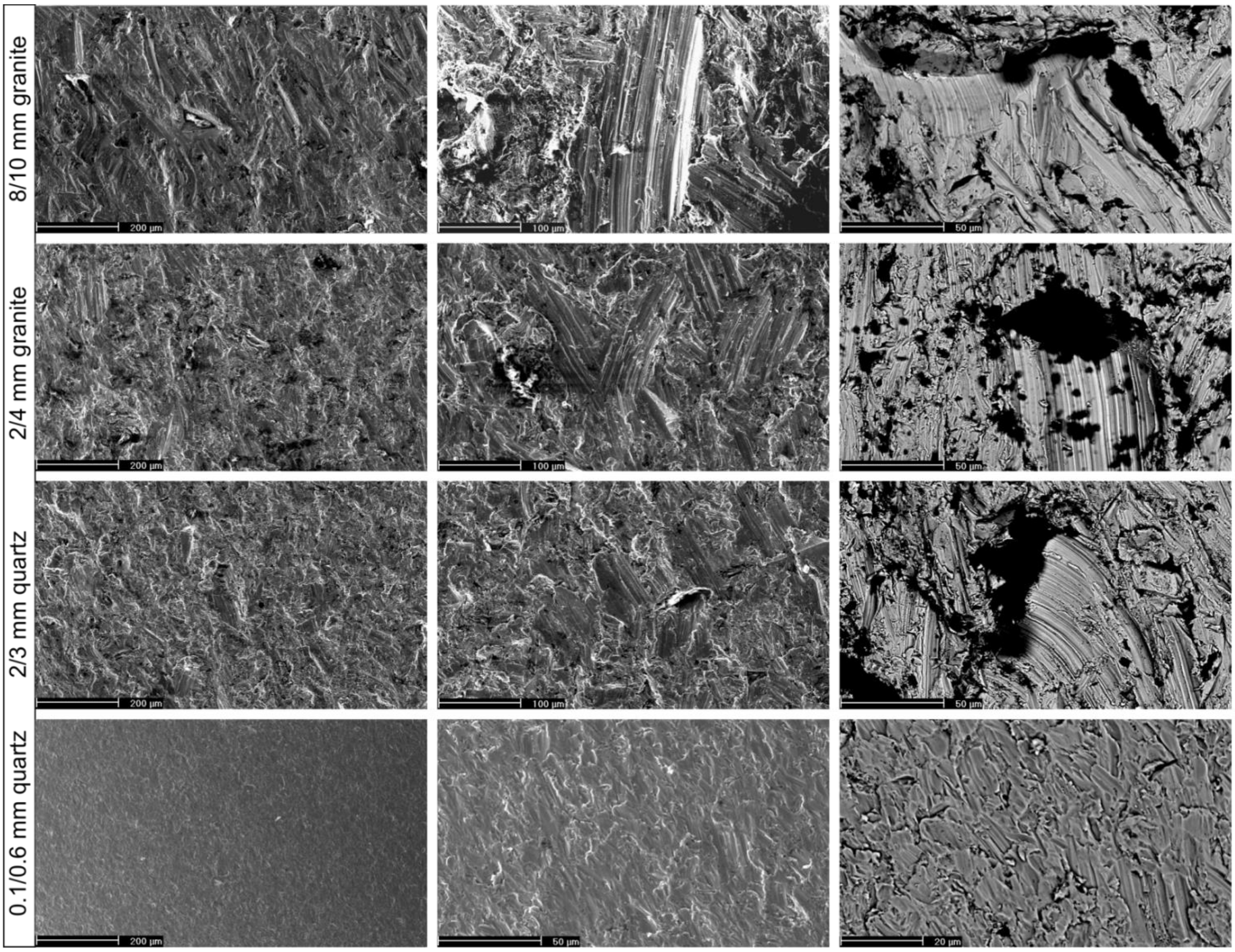


**Fig. 9 SEM images of the 400HB steel tested with different abrasives using a slurry concentration of 33 wt% and sample angle of 45°. On the left is a general overview with 100x magnification (scale bar 200 µm), in the middle a closer view (200x, 50 µm) where embedded abrasives can be observed, and on the right BSE images (500x, 20 µm) showing the largest scratches**

Only small differences could be noted between the wear resistant steels, and on a general level, the wear surfaces looked the same for all of the steels. The reason for this could be the similarity of the steels, as they are similar in the chemical composition and the only evident difference is in their hardness. On the other hand, a previous study on the abrasive wear of different steels belonging to the same hardness grade showed more clear differences, regardless of hardness [25]. On a detail level, the clearest differences are in the amount of plastic deformation and sharp scratches: the harder the steel, the less deformation and the more visible the scratches. The effect of slurry concentration, i.e., 9 or 33 wt% with 8/10 mm granite, was mainly limited to the degree of general deformation of the surfaces and the amount of scratches and embedded abrasives. Otherwise the basic nature of the wear surfaces was similar for both studied concentrations and also for both sample angles.

With the smallest particle size, only a couple of distinctive features could be observed for the tested steels, i.e., short and shallow scratches and limited mixing of the abrasives with the steel material. In general, the wear surfaces produced by the fine quartz were smooth and basically covered only by really short (ca. 10-20 µm) and narrow (ca. 2-5 µm) scratches. On the other hand, the average scratch width produced by the coarser quartz particles of 2/3 mm in size was similar to that produced by the 2/4 mm granite slurry, being about 40 µm at widest. With the most abrasive slurry used in the present tests, i.e., the 8/10 mm granite slurry, scratch widths up to about 100 µm were observed.

Fig. 10 presents details of the wear surface features observed in the steels tested with the largest particle size, i.e., plastic deformation, lip formation, and scratching. All of those are typical evolution steps of abrasive erosion wear for steels. While plastic deformation and scratching were common for all steel wear surfaces produced by particles over 2 mm in size, the lip formation was mainly present in the most abrasive conditions, i.e., the 33 wt% concentration of 8/10 mm granite slurry. Such lips are not anymore firmly attached to the surface, since there is abrasive or abrasive-steel composite material between the formed lip and the steel surface.

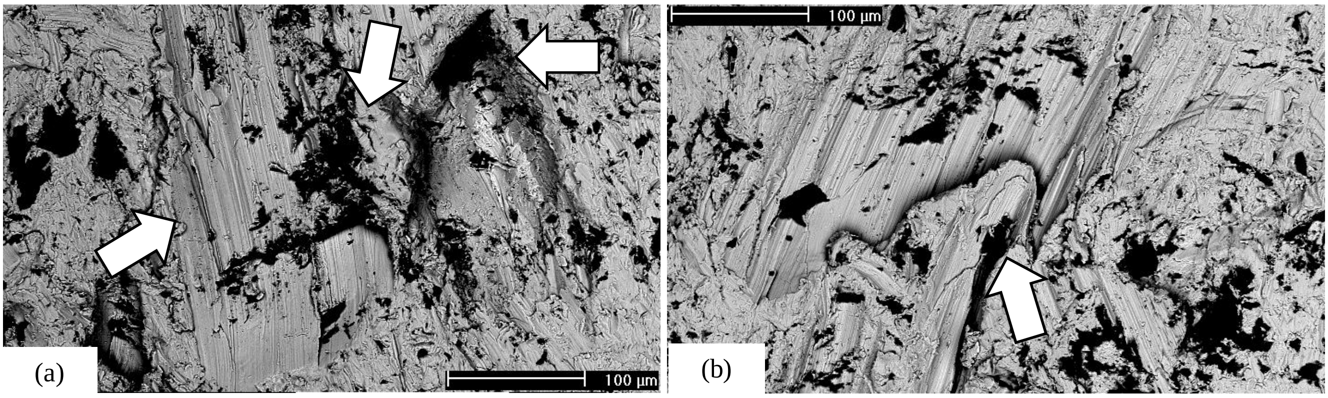


**Fig. 10 SEM BSE images of wear surface details after tests with 8/10 mm granite slurry at 45° sample angle of a) 500HB steel, showing a wide scratch, ploughing and embedded abrasives (marked with arrows), and b) 400HB steel, showing a wide scratch and a lip formed partly on top of it (marked with an arrow)**

Fig. 11 presents the wear surfaces of elastomers NR and PU2 produced by 33 wt% slurry containing fine quartz or large granite abrasives. With the 0.1/0.6 mm particle size, the wear surfaces are almost intact except for small scratches and some intended or attached abrasive particles. NR had the highest amount of particles on its wear surface. These particles were also the largest, up to 100 µm in diameter, which are four to five times larger than with the other elastomers. With 8/10 mm particle size, the surfaces were severely deformed. Larger scratches, dents and embedded abrasives were also frequently observed. With all test parameters, the surface of NR was clearly the roughest, having two (Fig. 11b) to five (Fig. 11a) times higher measured roughness compared to PU2.

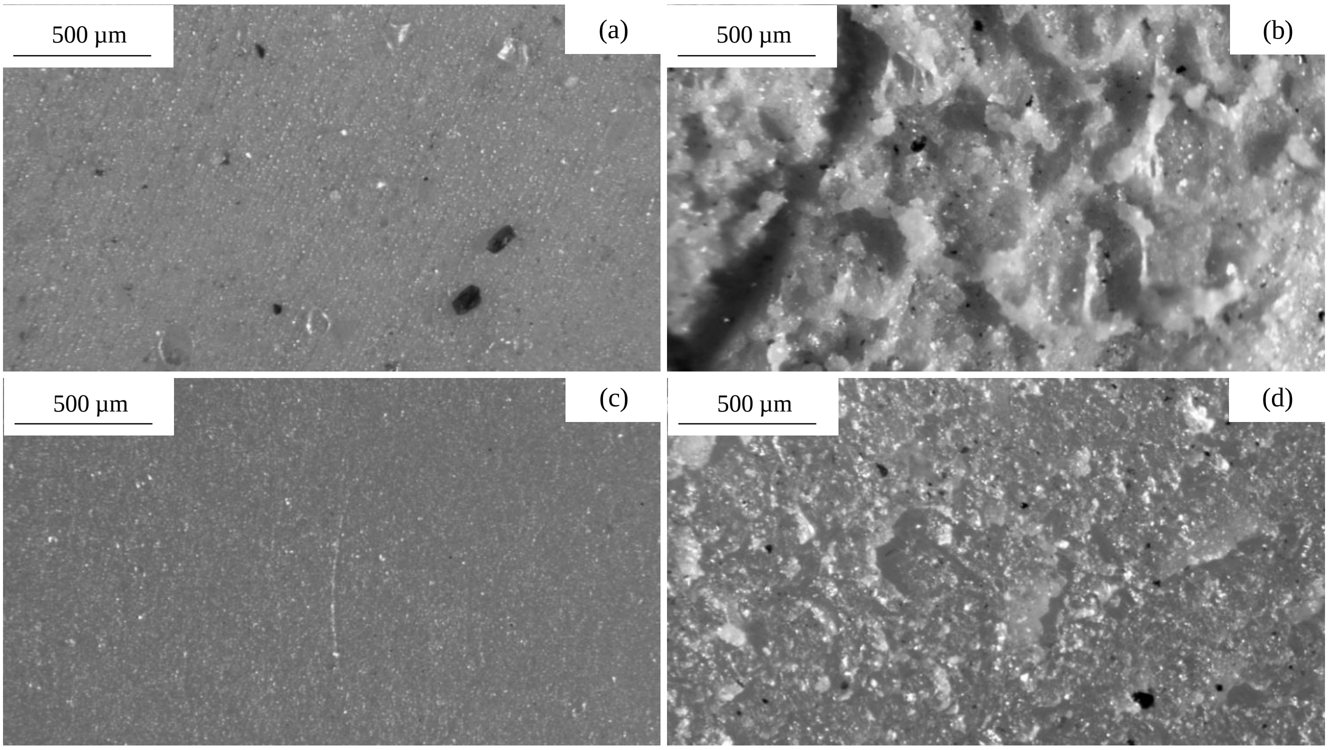


**Fig. 11 Wear surfaces of natural rubber (a and b) and PU2 polyurethane (c and d) tested with 33 wt% 0.1/0.6 mm quartz slurry (a and c) and 33 wt% 8/10 mm granite slurry (b and d) at 45° sample angle**

Fig. 12 presents a massive tear mark produced by 8/10 mm granite particles on the leading edge of a NR sample in a test with the 45° sample angle. The base plate steel was exposed under the approximately 4 mm wide piece of rubber that was already partly detached from the base plate.

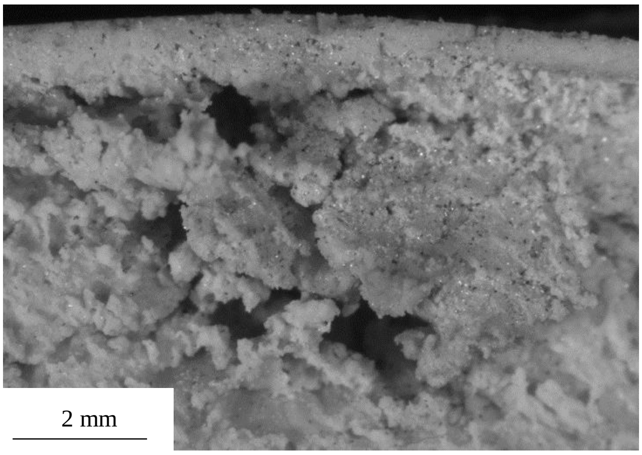


**Fig. 12 A large piece of the leading edge of the natural rubber sample, almost torn apart after a test with 33 wt% 8/10 mm granite slurry at the 45° sample angle**

## 3.3. Wear surface cross-sections

The surface deformations were studied more closely from the wear surface cross-sections of the wear resistant steel samples. In abrasive conditions, the most visible difference between the quenched steels was that while all of them showed similar deformed surface layers with white layers and shear bands, their size and quantity varied according to the hardness of the steel: the softer the steel, the more and larger the plastically deformed layers, such as white layers, and the harder the steel, the more and larger the shear bands. Fig. 13 shows a white layer and a shear band on the surface near the sample tip of the 400HB steel tested with 8/10 mm granite at a 90° sample angle. At the sample tip no big differences were observed between the sample angles, but further away from the tip some differences did exist. In a similar manner as the surface of the sample was observed to deform more at the 45° angle, in the cross-sections the deformation was found to extend deeper into the material.

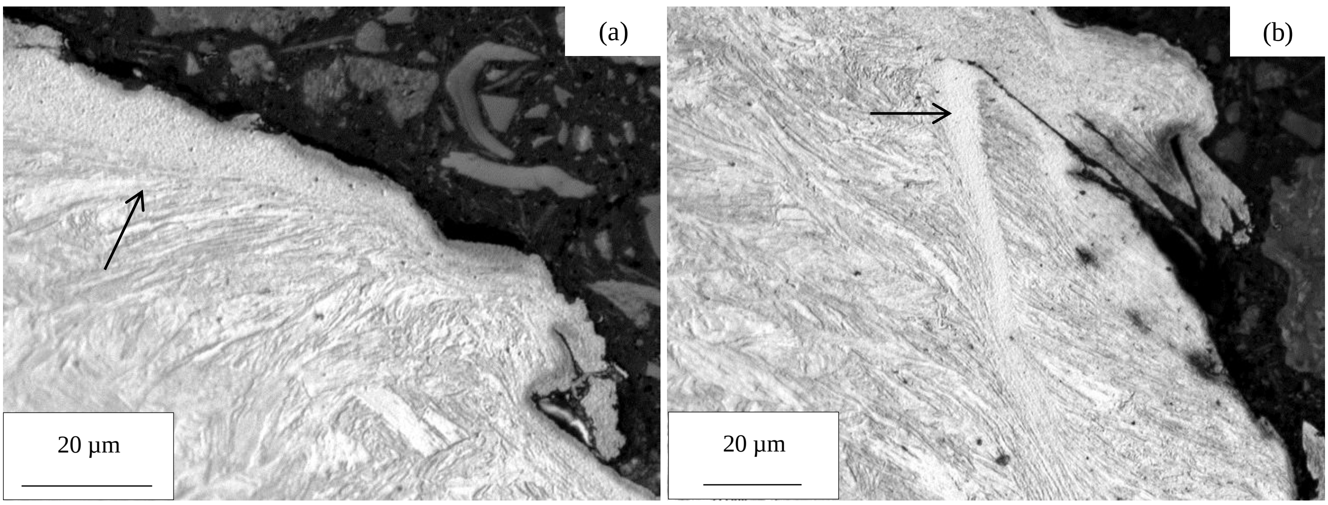


**Fig. 13 Surface deformation near the tip of a 400HB steel sample tested with 8/10 mm granite slurry showing a) a white surface layer and b) a shear band, both marked with arrows**

Intense and localized deformation can lead to the formation of hard surface layers and shear bands, which have a very fine microstructure and high hardness. The hardness difference compared with the surrounding material may lead to cracking and/or inability of the material to deform. The microhardness measurements carried out on the shear band shown in Fig. 13 revealed that in the top part of the band the hardness was as high as 760 HV25gf and stayed above 700 HV25gf, while the bulk hardness of the sample was 455 HV25gf. The hardest 500HB steel contained more shear bands than the softer ones, but only thin deformed surface layers. Fig. 14 presents a shear band that has branched near the surface. At the tip of the band, the measured hardness was as high as 820 HV25gf, while the bulk hardness was 590 HV25gf.

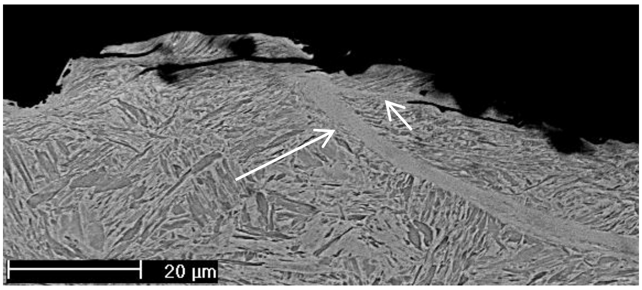


**Fig. 14 SEM image of a 500HB sample showing a branched shear band and lack of large surface deformations**

As the highly deformed and thus highly hardened surface layers eventually become markedly less ductile than the base material, it is possible that the wear performance of the steel significantly decreases. For example, in the cross-section of the 500HB steel tested with the 33 wt% 8/10 mm granite slurry, such brittle behavior was observed. Fig. 15 presents the result of a series of successive events on the wear surface that have led to the brittle cutting of the deformed surface layer. The events may have been the following: 1) a multitude of impacting abrasives have deformed and hardened the surface layer, 2) a larger abrasive particle, marked by the arrow on the left in the figure, have ploughed a part of the surface layer to form a lip, and 3) other particles have formed a scratch going over the deformed lip and cut a part of it. Similar cutting action was observed also in conjunction with the near surface shear bands, as presented in Fig. 14.

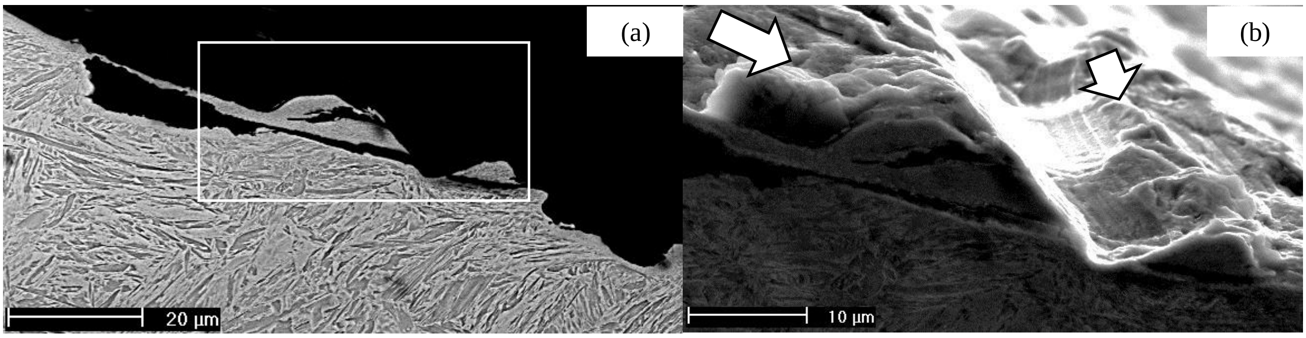


**Fig. 15 Cross-section of a 500HB steel sample tested with 33 wt% 8/10 mm granite slurry at 45° sample angle. a) SEM BSE image of the plastically deformed surface layer and b) SEM SE image of a stepwise formed scratch that has cut through the deformed surface layer**

In contrast, with fine quartz slurry the cross-sections appeared really smooth. In fact, in the 500HB steel it was almost impossible to see any deformation layer on the surface after the tests with fine quartz. In the 400HB steel, however, it was possible to observe 1-2 µm thick mixed layers of the deformed layer and a tribolayer composed of a mixture of the abrasive and the steel, as can be seen in Fig. 16. Also the microhardness measurements indicate the lack of plastic deformation and strain hardening of the wear surfaces, measured hardness being essentially the same before and after the test.

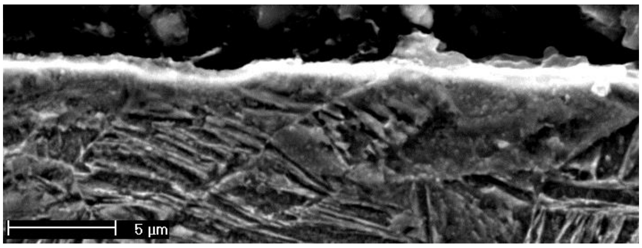


**Fig. 16 SEM SE image of a wear surface cross-section of the 400HB steel tested with 33 wt% 0.1/0.6 mm quartz slurry at 45° sample angle**

For the elastomers, the abrasive embedment was tried to analyze with x-ray computed tomography equipment. Fig. 17 presents a result for one NR sample. The faint veil on top is a wax layer used to fix the sample, so the surface of the sample is shown with the concentration of the bright spots. Density of the abrasive particles and usual filler materials used in the elastomers is the same, all between 2 and 3 g/cm$^3$, and that prevented a proper analysis of the embedment. But what can be observed is the concentration on the surface, and the rather homogenous spread after that. This means that the abrasive particles did penetrate only the very surface. As was the case with the steels also. Polyurethanes smaller embedding depth than the natural rubber.

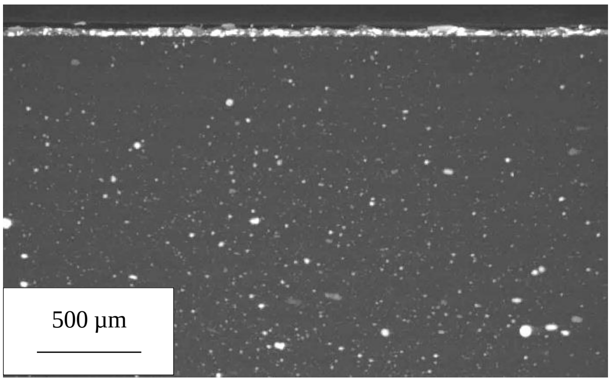


**Fig. 17 X-ray image of NR sample tested with 33 wt% 2/3 mm quartz slurry at 45° sample angle**

# 4. DISCUSSION

The industrial slurry erosion wear environments, such as in slurry transportation or dredging applications, are highly complex and in practice often only partly controllable [3]. Simulation of such processes or the wear performance of the materials in them with a laboratory test without similar complexity is not possible. This was the starting point for the application oriented wear testing performed in this study with the slurry-pot tester [9,18].

Slurry erosion tests were performed on several steels and elastomer materials in various slurry conditions. The tests proved that the abrasivity of the slurry is of key importance when the steels and elastomer materials are compared with each other. In this study the changes in abrasivity were achieved mainly by increasing the size of the abrasives, as the sample angle did not produce any notable difference when the other test parameters were constant. Larger abrasives have higher kinetic energy and will therefore induce more mass loss in the samples [11]. For ductile materials, such as the materials used in this study, the larger abrasive particle size promotes abrasive wear mechanisms such as cutting, as seen in Fig. 9 for the 400HB steel.

Relative wear performance increased for the steels with increasing abrasivity, i.e. particle size or slurry concentration, while for elastomers opposite performance was observed. In highly abrasive slurry erosion with large particles, where the kinetic energy of the abrasive particles was the highest, the quenched steels were on average 20 – 500 % better than the tested elastomers with 33 wt% concentration and 70 – 300 % better with 9 wt%

concentration. On the other hand, with fine 0.1/0.6 mm particles the steels were on average 70 – 90 % poorer than the elastomers. Visual inspection of all samples showed that the steels suffered much more extensive edge wear than the elastomers, especially natural rubber. This is evidently due to the much higher ability of the elastomers to deform elastically, or even deflect the particles in the case of the softest elastomers, without material loss under the slurry flow.

Within the two material types tested some mutual differences can be observed. Where the steels behaved linearly, mutual wear performance differences being 30 – 140 % depending the test conditions, the mutual behavior of elastomers did change radically after the fine quartz. While all elastomers were inside the same 30 % as the steels at minimum, the difference grew to over 800 %. It is interesting that the biggest difference between the elastomers was with coarse quartz slurry, as the difference between the steels was at minimum with that slurry. It is also notable that mutual ranking of the elastomers did change for the largest abrasive, PU2 being clearly second best elastomer.

Based on the wear surface characterizations, in the current tests the basic wear mechanism of the quenched steels was the same irrespective of the abrasive particle size, involving abrasive scratching and impact mark formation by repeated and continuous impacts of the particles, except for the fine quartz, with which the mechanism was mainly low-stress cutting. The difference between the steels arises only from the degree of deformation and abrasive scratching, i.e., from the different kinetic energy of the particles available in different test conditions. For the elastomers, the wear mechanism was mainly abrasive cutting and tearing, which was the reason for the notable rise of wear losses when moving from fine to large particle sizes. Elastomers also showed a high degree of abrasive particle penetration into the wear surfaces.

## 4.1. Abrasive slurry erosion and affecting factors

Based on the results of the wear tests and wear surface characterizations, the transition zone from low-stress to high-stress abrasive slurry erosion can be placed between 1-2 mm in terms of the abrasive particle size at the current sample speed. A clear change in the wear rate was also noted in terms of slurry concentration with the large 8/10 mm particle size. For the quenched steels the transition to larger concentration followed a similar slightly descending trend as found in a previous study for an austenitic stainless steel [11].

The two abrasives included in this study behaved differently during the tests, quartz being harder but also more brittle than granite. In any case, both abrasives are harder than the hardest of the tested steels and therefore capable of causing scratching in all of them. However, as granite is a heterogeneous rock consisting of different minerals, its average hardness is close to the highest hardness values measured for any of the studied quenched steels. On the other hand, the hardness of the homogenous quartz abrasives is notably higher than that of the steels in any stage of use, regardless of the degree of surface hardening, making even the smallest particle size relatively erosive for the steels. The brittleness of quartz leads to higher comminution of the abrasives during the test, which seems to increase the degree of particle penetration into the elastomer surfaces, as sharper and smaller particles can penetrate the soft elastomer surface more easily than the larger ones.

## 4.2. Mechanical behavior and wear performance of quenched steels in abrasive slurry erosion

The combination of high hardness and reasonable ductility enables the quenched wear resistant steels to be used in a wide variety of applications. For the progress of abrasive wear and the wear performance of the steels, a very important factor is the deformation behavior of the surface layers. It was found in this study that the deformation and work hardening of the wear surfaces of the wear resistant steels was negligible when tested with the fine quartz particles, 0.1/0.6 mm in size. However, with the largest particles of 8/10 mm in size, the surface hardness of the steels was increased by work hardening up to 20 % in the most deformed areas. On the other hand, as observed in several earlier studies on abrasive wear [25,29,30], strong work hardening is not always beneficial because it may lead to a detrimental loss of ductility on the surface of the steel. Similarly, in the current study on abrasive slurry erosion, it was observed that the strongly hardened surface layers can become brittle and be then cut away, as shown for example in Fig. 15b.

Microhardness measurements from the cross-sections showed that the quenched steels were all strain hardened to an extent that could be expected based on their yield/tensile strength ratios and remaining deformability. The steels, however, showed different deformation depths, as seen from the cross-sections prepared after the tests: the 400HB steel showed deformation depths up to 40 µm but the 500HB steel only up 10 µm, if any. The microhardness measurements indicated the same difference, as the 500HB steel showed descending near surface hardness gradients but the 400HB steel, instead, initially increasing gradients below the wear surface. Moreover, with the shallow deformation depths in the 500HB steel, the near surface areas cannot orient to adapt for the surface stresses.

Increasing brittleness or exhausted deformability, even to some limited extent, combined with the thin deformation layer of the 500HB steel may explain the deviation from the otherwise linear hardness dependence of wear performance and a possible change towards relatively poorer wear performance (Fig. 4). A similar change can also be observed in the dry impact-abrasion results published for similar steels by Ratia et al. [31]. However, plotting volume loss against 1/H, used in all equations modeling abrasion wear, the effect diminishes.

In a previous study with several 400HB grade quenched steels tested in high-stress dry abrasion conditions [25], some of the steels showed mechanical behavior resulting in a thin deformation layer and low deformation depth, while some other steels showed more ductile behavior with deeper deformations and oriented near surface structures. Both studies indicate that the extensively hardened surface layer with small deformation depths can lead to higher material losses in high-stress conditions because of the increased brittleness and sharp transition between the bulk material and the surface layer. In this study this means that while the deformability of the surface layer of all steels was equally consumed by abrasive erosion, the ductility and strain hardenability of the base material determines the total depth of deformation and thus the possible degree of the near surface re-orientation of the microstructure. Strain hardenability for these steels is mostly controlled by their carbon content, that increases towards the higher harness grades, and possibly by microalloying also, as normally for example Si, Ni, Mo contents also increases.

# 5. CONCLUSIONS

In this study, an abrasive slurry erosion wear comparison of quenched wear resistant steels and elastomer reference materials was performed. As pumping of slurry through pipelines is an increasingly more profitable alternative for transporting for example minerals or slurry away from mines or dredging sites, the technological boundaries in terms of wear resistance of the materials involved must be pushed forward. When the size of the abrasive particles exceeds 1-2 mm, high-stress abrasive wear becomes dominant, leading to a subtype of slurry erosion called abrasive slurry erosion. With increasing abrasivity, the role of corrosion also becomes smaller. In such demanding abrasive slurry erosion conditions, the quenched wear resistant steels can compete with elastomers in wear resistance.

The high speed slurry-pot wear tester proved to produce consistent and reproducible wear test results also with plate samples. As the tester offers versatility in test environment and sample arrangements, it facilitates application oriented testing ranging from large particle slurry erosion in dredging to small particle slurry transportation. However, as the slurry-pot tester is batch operated, the comminution of wear particles during testing may lead to conditions that to some extent differ from those in real applications, which should be taken into account when planning the tests and interpreting and applying the test results for example in materials selection and design of mineral handling and transportation machinery.

The studied wear resistant steels were similar except for their different hardness grades. Due to the similarities in the alloying and microstructure, the wear performance of the steels depended relatively linearly on the surface hardness. Nevertheless, some differences in the mechanical behavior of the studied steels could be noted. A clear transition from low-stress to high-stress abrasive slurry erosion was observed between the two quartz abrasives, which represented the smallest particle sizes in the tests. Based on the wear surface characterizations, the active wear mechanism in the steels was classified as abrasion dominated impact wear, or abrasive erosion in general.

One of the main observations of this study is that in certain conditions the wear resistant steels can offer better wear performance against abrasive slurry erosion than wear resistant elastomers. However, in low-stress abrasive slurry erosion conditions produced by particles less than 1 mm in size, the steels suffer from the limited plastic deformation and resulting lack of work hardening. The larger edge wear effect of the steels compared to the elastomer materials, especially in low-stress conditions, can be related to the lower elastic modulus and thus higher flexibility of the elastomers, although also polyurethanes exhibited rather dramatic edge wear above a certain limiting abrasive size. The surface behavior of the studied quenched wear resistant steels showed similarities to the earlier observations made in dry high-stress abrasion conditions, with the added effect of impact wear in the form of white layers and shear bands.

# ACKNOWLEDGEMENTS

The work has been done within the FIMECC BSA (Breakthrough Steels and Applications) programme as part of the FIMECC Breakthrough Materials Doctoral School. We gratefully acknowledge the financial support from the Finnish Funding Agency for Innovation (Tekes) and the participating companies. The corresponding author would like to express his gratitude to Jenny and Antti Wihuri Foundation.

# REFERENCES

[1] L. Gittins, Hydraulic Transport of Solids - Wear in Slurry Pipelines, Wear Slurry Pipelines - BHRA Inf. Ser. 1 (1980).

[2] T. Da Silva, Interview - Slurry Pipelines: Exciting Technology Entering Period of Renaissance, (2012). http://ceo.ca/2012/10/10/slurry-pipelines-exciting-technology-entering-period-of-renaissance/ (accessed January 18, 2015).

[3] G.F. Truscott, Wear in pumps and pipelines, Wear Slurry Pipelines - BHRA Inf. Ser. 1 (1980).

[4] Y. Tan, H. Zhang, D. Yang, S. Jiang, J. Song, Y. Sheng, Numerical simulation of concrete pumping process and investigation of wear mechanism of the piping wall, Tribol. Int. 46 (2011) 137–144. doi:10.1016/j.triboint.2011.06.005.

[5] Basics in Minerals Processing, 6th ed., Metso Minerals, Inc., 2008.

[6] A. Ossa, Interview on 12.12.2013, (2013) Multiaceros, Chile.

[7] M. Begiristain, Interview on 11.4.2014, (2014) AMPO, Spain.

[8] N. Zhang, F. Yang, L. Li, C. Shen, J. Castro, L.J. Lee, Thickness effect on particle erosion resistance of thermoplastic polyurethane coating on steel substrate, Wear. 303 (2013) 49–55. doi:10.1016/j.wear.2013.02.022.

[9] N. Ojala, K. Valtonen, P. Kivikytö-reponen, P. Vuorinen, V. Kuokkala, High speed slurry-pot erosion wear testing with large abrasive particles, Finnish J. Tribol. (2015).

[10] P. Kulu, R. Veinthal, M. Saarna, R. Tarbe, Surface fatigue processes at impact wear of powder materials, Wear. 263 (2007) 463–471. doi:10.1016/j.wear.2006.11.033.

[11] N. Ojala, K. Valtonen, P. Kivikytö-Reponen, P. Vuorinen, P. Siitonen, V.-T. Kuokkala, Effect of test parameters on large particle high speed slurry erosion testing, Tribol. - Mater. Surfaces Interfaces. 8 (2014) 98–104. doi:10.1179/1751584X14Y.0000000066.

[12] B. Yu, D.Y. Li, A. Grondin, Effects of the dissolved oxygen and slurry velocity on erosion–corrosion of carbon steel in aqueous slurries with carbon dioxide and silica sand, Wear. 302 (2013) 1609–1614. doi:10.1016/j.wear.2013.01.044.

[13] B.T. Lu, J.F. Lu, J.L. Luo, Erosion–corrosion of carbon steel in simulated tailing slurries, Corros. Sci. 53 (2011) 1000–1008. doi:10.1016/j.corsci.2010.11.034.

[14] H.M. Clark, R.J. Llewellyn, Assessment of the erosion resistance of steels used for slurry handling and transport in mineral processing applications, Wear. 250 (2001) 32–44. doi:10.1016/S0043-1648(01)00628-7.

[15] Y. Yang, Y.F. Cheng, Parametric effects on the erosion–corrosion rate and mechanism of carbon steel pipes in oil sands slurry, Wear. 276-277 (2012) 141–148. doi:10.1016/j.wear.2011.12.010.

[16] N. Pereira Abbade, S. João Crnkovic, Sand–water slurry erosion of API 5L X65 pipe steel as quenched from intercritical temperature, Tribol. Int. 33 (2000) 811–816. doi:10.1016/S0301-679X(00)00126-2.

[17] M.. Stack, N. Corlett, S. Turgoose, Some thoughts on modelling the effects of oxygen and particle concentration on the erosion–corrosion of steels in aqueous slurries, Wear. 255 (2003) 225–236. doi:10.1016/S0043-1648(03)00205-9.

[18] R. Gupta, S.N. Singh, V. Sehadri, Prediction of uneven wear in a slurry pipeline on the basis of measurements in a pot tester, Wear. 184 (1995) 169–178. doi:10.1016/0043-1648(94)06566-7.

[19] G.R. Desale, B.K. Gandhi, S.C. Jain, Effect of erodent properties on erosion wear of ductile type materials, Wear. 261 (2006) 914–921. doi:10.1016/j.wear.2006.01.035.

[20] A. Neville, C. Wang, Erosion–corrosion of engineering steels—Can it be managed by use of chemicals?, Wear.

267 (2009) 2018–2026. doi:10.1016/j.wear.2009.06.041.

[21] B.W. Madsen, A comparison of the wear of polymers and metal alloys in laboratory and field slurries, Wear. 134 (1989) 59–79. doi:10.1016/0043-1648(89)90062-8.

[22] Y.I. Oka, H. Ohnogi, T. Hosokawa, M. Matsumura, The impact angle dependence of erosion damage caused by solid particle impact, Wear. 203-204 (1997) 573–579. doi:10.1016/S0043-1648(96)07430-3.

[23] Y. Xie, J. (Jimmy) Jiang, K.Y. Tufa, S. Yick, Wear resistance of materials used for slurry transport, Wear. 332-333 (2015) 1104–1110. doi:10.1016/j.wear.2015.01.005.

[24] G.W. Stachowiak, A.W. Batchelor, Abrasive, Erosive and Cavitation wear, in: Eng. Tribol., 4th editio, Elsevier, 2014: pp. 525–576. doi:10.1016/B978-0-12-397047-3.00011-4.

[25] N. Ojala, K. Valtonen, V. Heino, M. Kallio, J. Aaltonen, P. Siitonen, et al., Effects of composition and microstructure on the abrasive wear performance of quenched wear resistant steels, Wear. 317 (2014) 225–232. doi:10.1016/j.wear.2014.06.003.

[26] C.I. Walker, P. Robbie, Comparison of some laboratory wear tests and field wear in slurry pumps, Wear. 302 (2013) 1026–1034. doi:10.1016/j.wear.2012.11.053.

[27] V. Levonmaa, Interview on 17.2.2014, (2014) Aquamec Oy, Finland.

[28] V. Ratia, V. Heino, K. Valtonen, M. Vippola, A. Kemppainen, P. Siitonen, et al., Effect of abrasive properties on the high-stress three-body abrasion of steels and hard metals, Tribol. - Finnish J. Tribol. 32 (2014) 3–18.

[29] A.K. Jha, B.K. Prasad, O.P. Modi, S. Das, A.H. Yegneswaran, Correlating microstructural features and mechanical properties with abrasion resistance of a high strength low alloy steel, Wear. 254 (2003) 120–128. doi:10.1016/S0043-1648(02)00309-5.

[30] J.K. Solberg, J.R. Leinum, J.D. Embury, S. Dey, T. Børvik, O.S. Hopperstad, Localised shear banding in Weldox steel plates impacted by projectiles, Mech. Mater. 39 (2007) 865–880. doi:10.1016/j.mechmat.2007.03.002.

[31] V. Ratia, K. Valtonen, A. Kemppainen, V.-T. Kuokkala, High-Stress Abrasion and Impact-Abrasion Testing of Wear Resistant Steels, Tribol. Online. 8 (2013) 152–161. doi:10.2474/trol.8.152.